

ARTICLE



Genetic heterogeneity in hereditary hearing loss: Potential role of kinociliary protein *TOGARAM2*

Memoona Ramzan¹, Mohammad Faraz Zafeer¹, Clemer Abad¹, Shengru Guo¹, Daniel Owrang^{2,3}, Ozgul Alper⁴, Ahmet Mutlu^{5,6}, Tahir Atik⁷, Duygu Duman⁸, Guney Bademci¹, Barbara Vona^{2,3}, Mahmut Tayyar Kalcioğlu^{5,6}, Katherina Walz^{1,9,10} and Mustafa Tekin^{1,9}✉

© The Author(s), under exclusive licence to European Society of Human Genetics 2024

Hearing loss (HL) is a heterogeneous trait with pathogenic variants in more than 200 genes that have been discovered in studies involving small and large HL families. Over one-third of families with hereditary HL remain etiologically undiagnosed after screening for mutations in the recognized genes. Genetic heterogeneity complicates the analysis in multiplex families where variants in more than one gene can be causal in different individuals even in the same sibship. We employed exome or genome sequencing in at least two affected individuals with congenital or prelingual-onset, severe to profound, non-syndromic, bilateral sensorineural HL from four multiplex families. Bioinformatic analysis was performed to identify variants in known and candidate deafness genes. Our results show that in these four families, variants in a single HL gene do not explain HL in all affected family members, and variants in another known or candidate HL gene were detected to clarify HL in the entire family. We also present a variant in *TOGARAM2* as a potential cause underlying autosomal recessive non-syndromic HL by showing its presence in a family with HL, its expression in the cochlea and the localization of the protein to cochlear hair cells. Conclusively, analyzing all affected family members separately can serve as a good source for the identification of variants in known and novel candidate genes for HL.

European Journal of Human Genetics (2024) 32:639–646; <https://doi.org/10.1038/s41431-024-01562-6>

INTRODUCTION

Genetic heterogeneity is a well-known phenomenon in hearing loss (HL). It refers to the fact that variants in multiple genes can cause a phenotype, and different individuals may have different genetic variations that result in a particular trait [1].

Hereditary HL can be categorized as syndromic and non-syndromic, where syndromic HL is associated with additional phenotypic findings. Both types of HL are characterized by significant genetic heterogeneity. To date, there are over 5000 rare variants in more than 200 genes that have been identified to cause HL presenting it as a highly heterogeneous trait (<https://www.hgmd.cf.ac.uk/ac/> and <https://hereditaryhearingloss.org/>). Non-syndromic HL alone can be caused by variants in more than 120 different genes. While the most common inheritance pattern of HL is autosomal recessive, all inheritance patterns can be seen in affected families.

The identification of causal gene variants for HL has become relatively easy due to the use of next-generation sequencing including exome sequencing (ES) and genome sequencing (GS). However, genetic heterogeneity can make genetic testing and diagnosis challenging even in multiplex families [2].

The purpose of this study was to identify the molecular basis of HL in families where index cases could be explained with a variant in a known deafness gene, but the identified variant failed to resolve the etiology of HL in all affected family members. In this small but informative cohort, we report the identification of additional variants in known genes and in a candidate gene, *TOGARAM2*, that could explain the HL in all family members.

MATERIALS AND METHODS

Ethics statement and study participants

Four families were enrolled as part of a larger international cohort for the identification of novel genes involved in sensorineural HL. The study was approved by the Institutional Review Board (Protocol no. 20081138) at the University of Miami (USA), Ankara University Medical School Ethics Committee (Protocol no. 012413) (Turkiye), Local Ethics Committee of Istanbul Medeniyet University (Turkiye), and Goztepe Training and Research Hospital in Istanbul (Turkiye). Written informed consents were obtained from all participants and in the case of minors, it was obtained from parents. Audiological examinations were performed in a soundproof room for adults and hearing for infants and minors was tested as per standard procedures and guidelines [3]. Romberg and tandem gait tests were used to evaluate vestibular function. Medical history and biochemical

¹John P. Hussman Institute for Human Genomics, University of Miami Miller School of Medicine, Miami, FL, USA. ²Institute of Human Genetics, University Medical Center Göttingen, Göttingen, Germany. ³Institute for Auditory Neuroscience and Inner Ear Lab, University Medical Center Göttingen, Göttingen, Germany. ⁴Department of Medical Genetics, Antalya University Medical School, Antalya, Turkey. ⁵Department of Otolaryngology, Istanbul Medeniyet University School of Medicine, Istanbul, Turkey. ⁶Otorhinolaryngology Clinic of Goztepe Prof. Dr. Suleyman Yalcin City Hospital, Istanbul, Turkey. ⁷Division of Pediatric Genetics, Ege University School of Medicine, Izmir, Turkey. ⁸Department of Audiology, Ankara University Faculty of Health Sciences, Ankara, Turkey. ⁹Dr. John T. Macdonald Foundation Department of Human Genetics, University of Miami Miller School of Medicine, Miami, FL, USA. ¹⁰IQUIBICEN CONICET, Faculty of Exact and Natural Sciences, University of Buenos Aires, Buenos Aires, Argentina.

✉email: mtekin@med.miami.edu

Received: 25 May 2023 Revised: 25 January 2024 Accepted: 7 February 2024

Published online: 19 February 2024

tests were requested where required and participating families were willing to cooperate with follow-ups.

Genetic analysis

All the affected members from each family were initially screened for the presence of biallelic variants in *GJB2* (MIM 121011). We completed ES initially in the probands of each family using either Agilent SureSelect Human All Exon kit version 4 or 5 (Agilent, Santa Clara, CA, USA), or IDT xGen™ V2 (IDT, Coralville, IA, USA). Sequencing was performed at 100X paired-end on HiSeq 2000 and BGISEQ-500 platforms. We performed ES in a second affected individual (II:1) in family 2503 and GS for individuals III:5 from family 1596, and II:2 from family 2450. Library preparation for GS was performed either with Illumina® DNA PCR-free preparation kit or by an in-house PCR-free library preparation protocol at BGI Genomics. Sequencing of the samples was carried out using a BGISEQ-500 with paired-end 100 bp (PE100).

The data obtained was aligned against human GRCh37/hg19 genome assembly using Burrows-Wheeler Aligner (<http://bio-bwa.sourceforge.net>) and variant calling was done with GATK software package (<https://www.broadinstitute.org/gatk/>). The FASTQ files were analyzed with an in-house software GENESIS (<https://app.tgp-foundation.org>). Primarily, single nucleotide, indel, and copy number variants (CNVs) in all known deafness genes were analyzed. Variants were retained for further evaluation if they had an allele frequency of less than 0.01. Homozygous, heterozygous, hemizygous, and compound heterozygous variants were examined. The variants in all known genes for HL were analyzed using a larger list retrieved from hereditary hearing loss homepage (<https://hereditaryhearingloss.org/>) and OMIM. The list from OMIM was obtained with keywords deafness, hearing loss, or hard of hearing in the clinical synopsis of entries with a phenotype associated with a molecular cause. The ES data were re-examined if there was no potential variant identified in the known deafness genes. CNV analysis with ES data used CoNIFER v.02.2 with default parameters. It uses a singular value decomposition method to correct systematic biases and identifies a CNV call if the corrected signal reaches a predefined threshold at no less than three consecutive exons [4]. CNV analysis with GS data used Manta, Delly and CNVnator [5–7]. The pathogenicity of the variants was determined as per description by the ACMG and ClinGen Hearing Loss Expert Panel (HL-EP) specifications to the ACMG/AMP variant interpretation guidelines [8–10]. Web tools such as GeneMatcher [11] were used to find additional probands with any candidate gene/variant. All novel variants identified were submitted to ClinVar.

We performed additional pathogenicity prediction for a missense Variant of Uncertain Significance (VUS) with a high CADD score (>20) by evaluating change in Gibbs free energy ($\Delta\Delta G$ in kcal/mol) [12]. Briefly, we obtained 3D protein structures from partial sequence of respective protein using AlphaFold2 which were refined using Galaxy Webserver (<https://galaxy.seoklab.org>). ProSA-web (<https://prosa.services.came.sbg.ac.at/>) and ERRAT (<https://saves.mbi.ucla.edu/>) were used for the validations of the final 3D models.

Change in free energy and its effect was predicted using DynaMut (<https://biosiglab.uq.edu.au/dynamut2/>), MUPro (<http://mupro.proteomics.ics.uci.edu/>) and CUPSAT (<http://cupsat.tu-bs.de/>). DynaMut uses protein structure as input and applies Normal Mode Analysis (NMA) for analyzing protein. However, it can also evaluate the effect of mutations on a protein stability using vibrational entropy changes. MUPro uses protein sequence as input and applies support vector machine (SVM) based methods to predict the effects of mutations based on $\Delta\Delta G$. CUPSAT is another structure-based tool that calculates the effect of point mutations on protein stability by applying the protein environment-specific mean force potentials. These potentials are extracted from the statistical evaluation of various available protein structure data sets. The results of all servers are defined in terms of $\Delta\Delta G$ value, in which the negative value corresponds to the destabilizing effect of the mutant.

The co-segregation of respective variants of interest was performed by Sanger sequencing in all available family members. We used Enlis Genome Research software with default parameters (<https://www.enlis.com/>) to analyze regions of homozygosity with ES or GS data. In individual II:2 of family 2450, we focused on variants mapping to homozygous regions after the excluding variants in known deafness genes.

Generation of *TOGARAM2* c.1543C>T variant in HEK293 cells

To generate patient-specific *TOGARAM2* variant c.1543C>T (p.Gln515Ter) in HEK293 cells, synthetic guide RNA (sgRNA) and HDR donor bearing the desired mutation were purchased from IDT (Table S1). HEK293 cells were obtained from ATCC (CRL-1573). Briefly, HEK293 cells were cultured to 80% confluency and Nucleofected with RNP complexes assembled at a

3.5:1 sgRNA to Cas9 ratio for 10 min at room temperature. The final concentrations of sgRNA, Cas9, and HDR donor were 140 pmol, 40 pmol, and 3 μ M, respectively. Nucleofection was performed using the 4D-Nucleofector system and SF Cell Line 4D-Nucleofector X Kit (Lonza, Cambridge, MA, USA Cat# V4XC-2012) according to the manufacturer's instructions. After nucleofection for 48 h, cells were cultured in advanced DMEM/F12 supplemented with 10% FBS and 1X antibiotic-antimycotic solution, along with 1 μ M of the HDR enhancer-V2 (IDT). Subsequently, HEK293 cells were maintained in their normal medium, i.e., DMEM supplemented with 10% FBS and 1X antibiotic-antimycotic, until ready for passage. At this stage, the CRISPR/Cas9-generated HEK293-*TOGARAM2* mutant cell pool was collected for cryopreservation and knock-in efficiency analysis by Sanger sequencing. DNA isolation was performed using QuickExtract™ DNA Extraction Solution (Lucigen LLC, Madison, WI, USA) according to the manufacturer's protocol, and subsequent Sanger sequencing and ICE analysis [13] were conducted using specific primers flanking the CRISPR/Cas9 PAM site (Table S1).

Following confirmation by Sanger sequencing, monoclonal isolation from the *TOGARAM2* (c.1543C>T) mutant pools was performed by limiting dilution to generate an isoclonal cell population. Limiting dilution plating aims to distribute cells in a 96-well plate at a concentration of 0.8 cells per 100 μ L per well, increasing the chance of obtaining one cell per well and reducing the likelihood of multiple cells in a single well. The limiting dilution plates were fed every other day, and once most of the colonies reached approximately 70% confluency, they were harvested. This was done by trypsinization, and the resulting cell suspension from each well was divided, with half cryopreserved and the other half used for confirmation via Sanger sequencing. To maintain clonality, care was taken to trypsinize only one clone at a time to reduce any risk of cross-contamination.

Quantitative reverse transcription PCR (qRT-PCR)

RNA was extracted from three monoclonal isogenic controls and three monoclonal *TOGARAM2* (c.1543C>T) knock-ins using TRIzol™ reagent following the manufacturer's protocol (Thermo Fisher Scientific, Rockville, MD, USA Cat# 15596026). Reverse transcription to synthesize cDNA was performed with qScript XLT cDNA SuperMix (Quantabio, Beverly, MA, USA) according to the manufacturer's instructions, using 1 μ g of RNA from each sample. The SYBR Green-based mRNA expression analysis for *TOGARAM2* was conducted on a QuantStudio 6 system (Thermo Fisher Scientific) with gene-specific primers 5'-ACGCTCAGCTAACTCATTAC-3' and 5'-GAAAGGCCTCAACTCCTTACA-3'. *HPRT1* was employed as an internal control, using primers 5'-CGAGATGTGATGAAGGAGATGG-3' and 5'-TTGATGTAATCCAGCAGGTGAC-3'.

Antibody validation

The sensitivity of rabbit polyclonal anti-*TOGARAM2* antibody (Abnova, Cheyenne, WY, USA Cat# PAB23133) was tested and validated in HEK293 *TOGARAM2* c.1543C>T knock-in cells (clone 20). Cells were grown to 70% confluency in DMEM supplemented with 10% FBS and 1X antibiotic-antimycotic at 37 °C with 5% CO₂. Cells were transfected with c-HA-*TOGARAM2* expression plasmid (GeneCopeia, Rockville, MD, USA EX-Y5496-M07) using jetPRIME transfection reagent (Polyplus, Illkirch-Graffenstaden, France). After 72 h, cells were fixed with 4% paraformaldehyde (PFA) in PBS for 30 min at room temperature, permeabilized with 0.5% Triton X-100 in PBS for 10 min, and then co-stained with mouse monoclonal HA-tag and rabbit polyclonal *TOGARAM2* primary antibodies overnight. The following day, cells were incubated with anti-mouse Alexa Fluor 488 and anti-rabbit Alexa Fluor 555 secondary antibodies, respectively. Subsequently, the cells were counterstained with DAPI and mounted in Prolong Gold antifade solution (Invitrogen, Rockville, MD, USA). Images were acquired using a 63x objective on a Zeiss LSM710 confocal microscope (Carl Zeiss, OKO, Germany).

Togaram2 expression in mice

All procedures involving animals were approved by the University of Miami Institutional Animal Care and Use Committee (Protocol no. 23-144) followed by National Institutes of Health (NIH) guides, 'Using Animals in Intramural Research'.

Quantitative PCR was used to assess mouse expression levels of *Togaram2* in cochlea from postnatal day 0 (P0), 15 (P15), and 30 (P30). Additionally, expression of *Togaram2* was examined in various other tissues, including the hippocampus (Hi), cortex (Cx), liver (Li), spleen (Sp),

kidney (Ki), and lung (Lu) from postnatal P30. RNA was isolated from the mentioned tissues using TRIzol (Invitrogen). One microgram of RNA was used to synthesize cDNA using qScript XLT cDNA SuperMix (Quantabio). The primers utilized to amplify a 411 bp fragment of *Togaram2* were as follows: Forward 5'-CATGGCGGCATCTTCTCAAG-3' and Reverse 5'-GCCTTTGGTCCATAAGCAC-3'. For *Gapdh* a 129 bp fragment was amplified using the following primers: Forward 5'-AGGTCGGTGTGAACG-GATTG-3' and Reverse 5'-TGAGACCATGTAGTTGAGGTCA-3'.

To assess TOGARAM2 specific localization, whole-mount immunofluorescence of the organ of Corti was performed using P1 mouse cochlea. The dissected cochlea was fixed in 4% PFA, and permeabilization was done using 0.25% Triton X-100, blocking for 1 h in 5% BSA, and incubated overnight at 4 °C with primary antibodies. Rabbit polyclonal anti-TOGARAM2 antibodies ab122395 (Abcam, CB, UK) or PAB23133 (Abnova) were used as indicated in results due to discontinuation of the Abcam antibody during the research period, mouse monoclonal anti-Acetylated α -Tubulin antibody (Millipore, Burlington, MA, USA Cat# T7451), and mouse monoclonal anti-RAB11 antibody (BD, Franklin Lakes, NJ, USA Cat# BD610656) were utilized as primary antibodies. Immunolabeling of the anti-TOGARAM2 antibody was performed using goat anti-rabbit Alexa fluor 488, goat anti-mouse Alexa fluor 568 for Acetylated α -Tubulin and RAB11. Alexa fluor 647 Phalloidin (Thermo Fisher Scientific Cat# A22287) was used to counterstain the actin filaments in stereocilia. All specimens were mounted with a fluorescence mounting medium (Dako, Glostrup, Denmark). Confocal images were acquired using 63x objective on LSM 710 Zeiss confocal microscope (Carl Zeiss).

Scanning Electron Microscopy (SEM)

Dissected cochleae were placed in 1X PBS containing 2% glutaraldehyde. The samples were rinsed for five minutes each in 1X PBS. Cochleae were then post-fixed with 0.01 M osmium tetroxide for 2 h and then rinsed three times for five minutes each in PBS. Samples were dehydrated in a graded series to 100% and dried in hexamethyldisilane. Samples were coated with Palladium (Pd) in a sputter coater and imaged with an XL-30 field emission SEM.

RESULTS

All four families in this sub-cohort have congenital or prelingual onset, bilateral severe-profound HL (Table 1). In families 1596 and 2625, parents originated from the same small towns, and in family 2450, parents were first cousins. The detailed physical examinations in the probands and available family members showed no other clinical findings associated with HL in these families and Romberg and tandem walking were normal.

The initial analysis of ES data in the probands of this small cohort identified variants in four known deafness genes. One of the pathogenic variants was present in *MARVELD2* (MIM 610572) previously known as *TRIC* (tricellulin) due to its presence at tricellular junctions of three epithelial cells [14], and other variants were in *SOX10* (MIM 602229), *COL11A2* (MIM 120290), and *MYO15A* (MIM 602666). However, upon segregation analysis, these variants did not explain HL in all members of the same family (Fig. 1A, B). The additional ES/GS of unsolved family members revealed variations in a second deafness gene in families 1596, 2503, and 2625, following a careful analysis of variants in all known deafness genes, including CNVs.

In family 1596, three of four affected siblings were homozygous for the pathogenic c.1331+2 T>C variant in *MARVELD2*. Individual III:5, who was heterozygous for the variant underwent GS, which identified a novel variant in *TECTA* (MIM 602574), c.569 C>T (p.Thr190Met) (SCV004022367). This variant has an aggregated allele frequency of 0.000002 in gnomAD (v4.0.0) and is absent in our internal database including 1,612 Turkish controls. Under ACMG and HL-EP guidelines this variant was classified as VUS. However, the additional predictions for $\Delta\Delta G$ suggest that it causes a destabilizing effect on the protein folding conformation (Tables S2 and S1). MAVERICK and AlphaMissense scores are 0.62 and 0.6403 (pathogenic) for the *TECTA* variant, respectively [15]. Individual III:4 in family 1596 was homozygous for both

variants in *MARVELD2* and *TECTA* without any difference in phenotypic presentation.

In family 2503, the proband (II:2) was homozygous for the pathogenic variant c.1334 T>G (p.Leu445Trp) in *SLC26A4*. Her affected daughter (III:1) was heterozygous for this variant. ES in the affected father (II:1) showed a likely pathogenic variant c.89G>T (p.Ser30Ter) in *SOX10*, for which the daughter was heterozygous as well. Further evaluation of the father and daughter, who were not available for phenotypic evaluation initially, showed pigmentary abnormalities in the eye; along with genotype data consistent with autosomal dominant Waardenburg syndrome (MIM 613266).

Individual II:3 from family 2625 was a homozygous for a likely pathogenic variant c.6551 G>A (p.Thr2184Met) in *MYO7A* (MIM 276903). However, only two of the four affected siblings were homozygous for this variant. The proband was also heterozygous for another likely pathogenic variant c.966dupC (p.Thr323HisfsTer19) in *COL11A2*. Sanger sequencing showed that three siblings were homozygous for the *COL11A2* variant. Individual II:4 was homozygous for both variants but there was no phenotypic difference compared to other siblings.

In family 2450, two of the three affected siblings were homozygous for a pathogenic *MYO15A* variant, c.4441 T>C (p.Ser1481Pro). GS in the affected sibling who does not have this variant (II:2) did not reveal a plausible variant in any known HL gene. Via GS, we detected 15 homozygous runs greater than 2 MB in this individual (Table S3). Only one known deafness gene, *OTOF* (MIM 603681), was lying in one of the homozygous regions on chromosome 2. The *OTOF* gene was covered with 100%, 99.9%, and 98.5% for the 1X, 5X, and 10X reads, respectively. The mean coverage of *OTOF* was 88X. Analysis of all the exonic and intronic regions of the gene with a minor allele frequency of 0.01 did not identify any variants that can associate *OTOF* with the phenotype. There was no CNV involving *OTOF* as well. We then searched for variants with allele frequency less than 0.007 as suggested by the ClinGen HL Group [9] and CADD>20 in the genes mapped to these homozygous regions. This analysis identified seven variants (Table S4). We subsequently applied MAVERICK to predict the pathogenicity and mode of inheritance of these variants. MAVERICK uses AI to classify variants based on their impact on the gene product and reported variations of a given gene. It was shown that a benign score >0.5 removes 98% of benign variants [16]. Three out of seven variants had <0.5 benign score including *KHK* (MIM 614058) c.259 G>A (p.Val87Ile), *TOGARAM2* c.1543 C>T (p.Gln515Ter) (SCV004022368), and *GRID1* (MIM 610659) c.1894A>C (p.Ile632Leu). *KHK* encodes ketoheokinase and biallelic variants in this gene were reported in essential fructosuria (MIM 229800), which is a benign metabolic condition without HL [17]. The *GRID1* variant is predicted to cause an autosomal dominant phenotype based on a MAVERICK score of 0.74 and a pLI score of 1. The *TOGARAM2* variant is absent in gnomAD and in our internal database which includes 1,612 Turkish individuals. It has an autosomal recessive MAVERICK score of 0.94, making this nonsense variant a promising candidate to explain HL in individual II:2. Finally, none of the other variants received a pathogenic score when we applied AlphaMissense predictions (Table S4).

The localization of the premature stop codon in *TOGARAM2* suggests that it can trigger nonsense-mediated mRNA decay (NMD) (Fig. 1C). We generated and confirmed 6 monoclonal wild type isogenic cell lines and 12 monoclonal *TOGARAM2* (c.1543 C>T) knock-in cell lines (Fig. S2). Preliminarily, via qRT-PCR, we showed that HEK293 cells express *TOGARAM2*. Subsequently, the comparative analysis of wild type and CRISPR-Cas9-mediated HEK293 cells showed that the variant significantly reduces the mutated mRNA, suggesting the presence of NMD (Fig. 2A, B).

The gEAR portal shows that *Togaram2* is expressed in the inner ear (<https://umgear.org/>), but the specific expression pattern of *Togaram2* in the organ of Corti has not been previously reported.

Table 1. Variants in more than one gene identified for hearing loss in participating families.

Family and individual ID	Hearing loss	Gene	HGVs variant	Variant type	Zygoty	ACMG/HL-EP classification	Pathogenicity classification	Reference
1596 III:1	Bilateral severe-profound	<i>MARVELD2</i>	NM_001038603.3 c.1331+2 T > C p.Cys395fsTer403	Splice region	Homozygous	PVS1_very strong, PM2_sup, PPI_strong	P	[30]
1596 III:5	Bilateral severe-profound	<i>TECTA</i>	NM_005422.4 c.569 C > T p.Thr190Met	Missense	Homozygous	PM2_sup, PM3_sup, PP3_sup, PPI_sup	VUS	none
2503 II:2	Bilateral severe-profound	<i>SLC26A4</i>	NM_000441.2 c.1334 T > G p.Leu445Trp	Missense	Homozygous	PM2_sup, PP3_strong, PPI_very strong, PS3_sup	P	[31]
2503 II:1	Bilateral severe-profound	<i>SOX10</i>	NM_006941.4 c.89 G > T p.Ser30Ter	Nonsense	Heterozygous	PVS1_strong, PM2_sup	LP	[32]
2625 II:1	Bilateral severe-profound	<i>COL11A2</i>	NM_080680.2 c.966dupC p.Thr323HisfsTer19	Frameshift	Homozygous	PVS1_strong, PM2_sup	LP	[33]
2625 II:3	Bilateral severe-profound	<i>MYO7A</i>	NM_000260.4 c.6551 G > A p.Thr2184Met	Missense	Homozygous	PM2_sup, PP3_mod, PPI_strong	LP	[34]
2450 II:1	Bilateral profound	<i>MYO15A</i>	NM_016239.3 c.4441 T > C p.Ser1481Pro	Missense	Homozygous	PM2_sup, PP3_strong, PPI_strong	P	[35]
2450 II:2	Bilateral profound	<i>TOGARAM2</i>	NM_199280.2 c.1543 C > T p.Gln515Ter	Nonsense	Homozygous	Candidate gene	Candidate gene	none

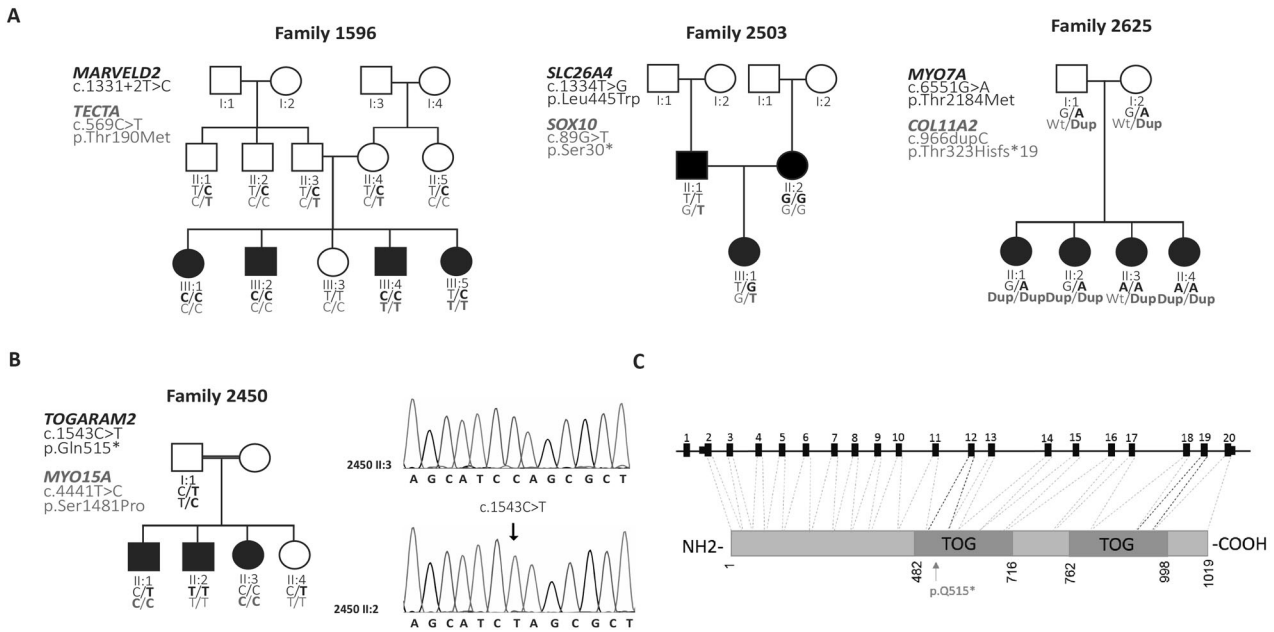


Fig. 1 Pedigrees depicting genetic heterogeneity and variants identified in deafness genes. **A** Pedigrees of all participating families with segregating known deafness gene variants. Clear symbols represent unaffected individuals while filled circles and squares denote affected individuals. **B** Segregation of *MYO15A* and *TOGARAM2* in family 2450. **C** Graphical representation of *TOGARAM2*. The gene consists of 20 exons which encode a large protein of 1019 amino acids. The variant p.Gln515Ter is located in a TOG-like domain of the protein.

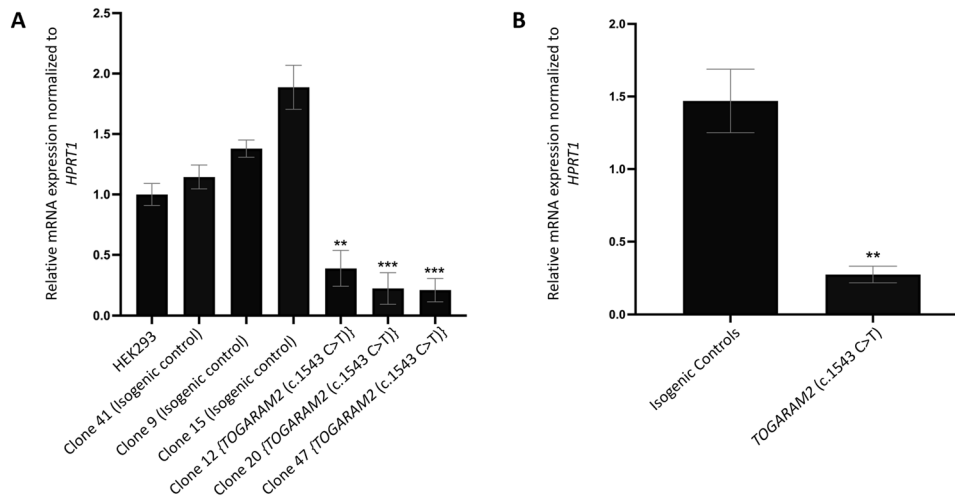


Fig. 2 In vitro analysis of c.1543C>T variant in *TOGARAM2*. **A** Quantitative mRNA expression levels of *TOGARAM2* in wild type isogenic monoclonal clones compared to monoclonal *TOGARAM2* (c.1543 C > T) knock-ins. Statistical analysis was performed using ANOVA, and data are presented as mean \pm SD normalized to *HPRT1* expression. Significant differences are indicated with an asterisk (** $p \leq 0.01$, *** $p \leq 0.001$) when compared to HEK293. **B** Overall quantitative mRNA expression levels of *TOGARAM2* in wild type isogenic clones versus *TOGARAM2* (c.1543 C > T) knock-ins. Statistical analysis was conducted using a student's t-test, and data are shown as mean \pm SD normalized to *HPRT1* expression. Significant differences are denoted with an asterisk (* $p \leq 0.01$) when compared to controls.

To study the specific localization of *TOGARAM2* in the organ of Corti, we performed immunofluorescence of the mouse cochlea with a validated antibody against *TOGARAM2* (Fig. S3) and an antibody against Acetylated α -Tubulin, which identifies the kinocilium. A representative image captured from the mid-turn cochlea shows the uniform distribution of *TOGARAM2* at the base of the kinocilium in both the outer and inner hair cells at different ages (Figs. 3A, B and S4). The pattern of expression for *TOGARAM2* was consistent with localization on the base of the kinocilium (Fig. 3C). To confirm this hypothesis, a co-staining with anti-RAB11 antibody, which serves as a marker for the base of kinocilium, was performed. As can be seen in Fig. 3D, *TOGARAM2* and RAB11 co-

localized, reinforcing the idea that *TOGARAM2* is among the proteins present at the base of the kinocilium.

To gain a more comprehensive understanding for the timing of *Togaram2* expression, we performed RT-PCR analysis on wild type mice. The *Togaram2* expression was examined in the cochlea at different time points: P0, P15, and P30. The results (Fig. S5) indicate that *Togaram2* mRNA is present at P0 but not at P15 or P30. This result correlates with the existence of the kinocilium at early life stages and supports the idea that *TOGARAM2* is specifically associated with this structure. The presence of *TOGARAM2* at P4 but not at P12 via immunostaining further supports this association (Fig. S4).

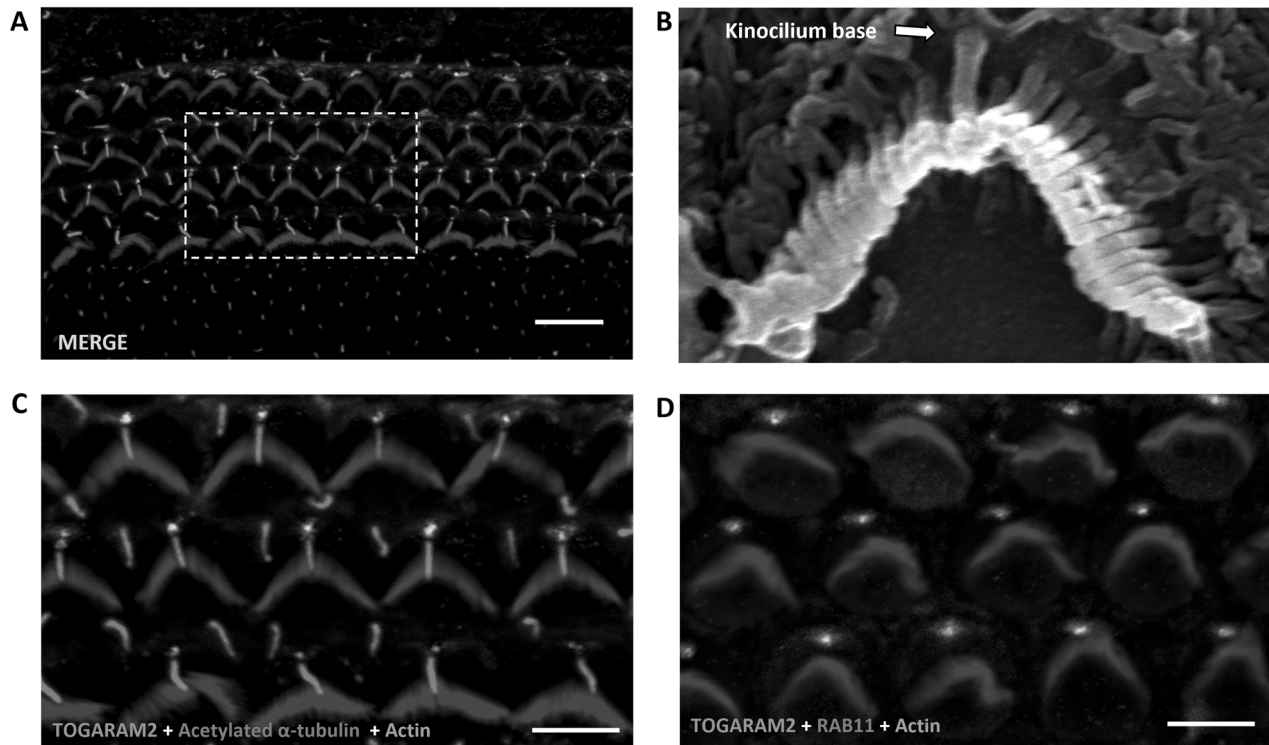


Fig. 3 Localization of TOGARAM2 in the cochlea from a P1 wild type mouse. **A** Merged view of a whole mount of the mid turn of the cochlea at P1 shows the protein localization at the basal body of the kinocilium in green, the kinocilium marked with acetylated α -Tubulin in red, and the stereocilia marked with actin in blue, of outer and inner hair cells. Scale bar: 10 μ m. **B** Representative image of stereocilia bundle using Scanning Electron Microscopy (SEM) from P4 animal indicating the base of kinocilium. **C** A higher magnification of the stereocilia bundles shown in **A** suggests that TOGARAM2 is present at the basal body of the kinocilium. Scale bar: 5 μ m. **D** A confocal magnified view of P1 wild-type whole mount cochlea showing RAB11 (red) and TOGARAM2 (green) colocalization at the base of kinocilium. Scale bar: 5 μ m.

DISCUSSION

The recognized genes associated with HL are involved in carrying out functionally relevant biological processes such as neuronal transmission, cell growth, differentiation and survival, cochlear homeostasis and ionic balance, hair cell organization and function, as well as cellular adhesion, demonstrating the complexity of the auditory system and the genetic heterogeneity of HL [18]. Discovery of the causative variants is crucial for proper clinical management, genetic counseling, and gene therapy, which is becoming available. Difficulties in the identification of causative variants arise due to complex family structures, phenocopies, and variable penetrance [19, 20]. In addition, extreme genetic heterogeneity, even among small families, has particularly made the diagnosis difficult. Previously, we have reported 161 small and large multiplex Turkish families where genetic heterogeneity was observed in 6% of families (10/161). We were able to secure genetic diagnosis for five of them [21] and this report, while others remained unsolved even after additional sequencing of available family members (Fig. S6). The presence of heterogeneity among consanguineous families can give rise to more complications regarding suitability for gene therapy trials. Our results suggest that each affected individual in multiplex families needs comprehensive genetic evaluation to find the causal variant/s.

The present study addresses the efficient use of ES/GS for family-based analysis of small families presenting with heterogeneity. We have identified rare variants in more than one known deafness gene segregating in a single family. Given the allelic spectrum and heterogenous nature of HL, our results correlate with several other studies that reported large families with variants in more than one gene causing HL [22–25].

In our cohort, an affected individual was found to be homozygous for a nonsense variant in TOGARAM2 (previously

known as *FAM179A*), which encodes a TOG array regulator of axonemal microtubules protein 2, exclusively present in mammals [26]. The TOGARAM2 variant (c.1543 C > T) leads to the reduction of mRNA, probably due to NMD, which is not likely to be sufficient to carry out proper functioning. TOGARAM2 is a large protein with 1019 amino acids and comprised of two TOG-like domains (Fig. 1C), which have sequence and structure similarity with TOG-3 and TOG-4 domains of the Crescerin1/FAM179B subfamily. Since TOG-3 and TOG-4 domains of Crescerin1/FAM179B are known to bind microtubules and are responsible for conformational changes in α -Tubulin [26, 27], we hypothesized that TOGARAM2 may also play a similar role of binding tubulin in ciliary structures. The localization of TOGARAM2 in the hair cell kinocilium of mouse inner ear also suggests its possible role in the organization of stereocilia. It has been shown that variations in different proteins involved in stereocilia function and organization can cause sensorineural HL [28, 29]. We thus present TOGARAM2 as a candidate gene for HL. Further, in vivo mouse studies to clarify the role of TOGARAM2 in hearing and deafness are underway, which we hope will be further supported through the identification of additional families with HL and biallelic variants as well as other functional studies.

List of URLs

Burrows-Wheeler Aligner (<http://bio-bwa.sourceforge.net>). GATK (<https://www.broadinstitute.org/gatk/>). GENESIS (<https://app.tgp-foundation.org>). Enlis Genome Research (<https://www.enlis.com/>). Galaxy Webserver (<https://galaxy.seoklab.org>). ProSA-web (<https://prosa.services.came.sbg.ac.at/>). ERRAT (<https://saves.mbi.ucla.edu/>). DynaMut (<https://biosig.lab.uq.edu.au/dynamut2/>). MUPro (<http://mupro.proteomics.ics.uci.edu/>). CUPSAT (<http://cupsat.tu-bs.de/>). OMIM (<https://www.omim.org/>). Hereditary

hearing loss homepage (<https://hereditaryhearingloss.org/>). UCSC (<http://genome.ucsc.edu>). gnomAD (<https://gnomad.broadinstitute.org/>). gEAR (<https://umgear.org/>).

DATA AVAILABILITY

All data generated or analyzed during this study are included in this article and its supplementary information files. The genetic variants are submitted to ClinVar database; accession IDs SCV004022367 and SCV004022368.

REFERENCES

- McGinniss MJ, Kaback MM. Heterozygote testing and carrier screening. Emery and Rimoin's principles and practice of medical genetics: Elsevier; 2013. p. 1–10.
- Pandya A, O'Brien A, Kovasala M, Bademci G, Tekin M, Arnos KS. Analyses of del (GJB6-D13S1830) and del (GJB6-D13S1834) deletions in a large cohort with hearing loss: Caveats to interpretation of molecular test results in multiplex families. *Mol Genet Genom Med*. 2020;8:e1171.
- Mazzoli M, Van Camp G, Newton V, Giarbini N, Declau F, Parving A. Recommendations for the description of genetic and audiological data for families with nonsyndromic hereditary hearing impairment. *Audiol Med*. 2003;1:148–50.
- Krumm N, Sudmant PH, Ko A, O'Roak BJ, Malig M, Coe BP, et al. Copy number variation detection and genotyping from exome sequence data. *Genome Res*. 2012;22:1525–32.
- Chen X, Schulz-Trieglaff O, Shaw R, Barnes B, Schlesinger F, Källberg M, et al. Manta: rapid detection of structural variants and indels for germline and cancer sequencing applications. *Bioinformatics*. 2016;32:1220–2.
- Rausch T, Zichner T, Schlattl A, Stütz AM, Benes V, Korb J. DELLY: structural variant discovery by integrated paired-end and split-read analysis. *Bioinformatics*. 2012;28:i333–i9.
- Abyzov A, Urban AE, Snyder M, Gerstein M. CNVnator: an approach to discover, genotype, and characterize typical and atypical CNVs from family and population genome sequencing. *Genome Res*. 2011;21:974–84.
- Richards S, Aziz N, Bale S, Bick D, Das S, Gastier-Foster J, et al. Standards and guidelines for the interpretation of sequence variants: a joint consensus recommendation of the American College of Medical Genetics and Genomics and the Association for Molecular Pathology. *Genet Med*. 2015;17:405–23.
- Oza AM, DiStefano MT, Hemphill SE, Cushman BJ, Grant AR, Siegert RK, et al. Expert specification of the ACMG/AMP variant interpretation guidelines for genetic hearing loss. *Hum Mutat*. 2018;39:1593–613.
- Tavtigian SV, Harrison SM, Boucher KM, Biesecker LG. Fitting a naturally scaled point system to the ACMG/AMP variant classification guidelines. *Hum Mutat*. 2020;41:1734–7.
- Sobreira N, Schiettecatte F, Valle D, Hamosh A. GeneMatcher: a matching tool for connecting investigators with an interest in the same gene. *Hum Mutat*. 2015;36:928–30.
- Tollefson MR, Gogal RA, Weaver AM, Schaefer AM, Marini RJ, Azaiez H, et al. Assessing variants of uncertain significance implicated in hearing loss using a comprehensive deafness proteome. *Hum Genet*. 2023;142:819–34.
- Conant D, Hsiao T, Rossi N, Oki J, Maures T, Waite K, et al. Inference of CRISPR edits from Sanger trace data. *CRISPR J*. 2022;5:123–30.
- Ikenouchi J, Furuse M, Furuse K, Sasaki H, Tsukita S, Tsukita S. Tricellulin constitutes a novel barrier at tricellular contacts of epithelial cells. *J Cell Biol*. 2005;171:939–45.
- Cheng J, Novati G, Pan J, Bycroft C, Žemgulytė A, Applebaum T, et al. Accurate proteome-wide missense variant effect prediction with AlphaMissense. *Science*. 2023;381:eadg7492.
- Danzi MC, Dohrn MF, Fazal S, Beijer D, Rebelo AP, Cintra V, et al. Deep structured learning for variant prioritization in Mendelian diseases. *Nat Commun*. 2023;14:4167.
- Bonthron DT, Brady N, Donaldson LA, Steinmann B. Molecular basis of essential fructosuria: molecular cloning and mutational analysis of human ketohexokinase (fructokinase). *Hum Mol Genet*. 1994;3:1627–31.
- Petit C. From deafness genes to hearing mechanisms: harmony and counterpoint. *Trends Mol Med*. 2006;12:57–64.
- Sirmaci A, Edwards YJ, Akay H, Tekin M. Challenges in whole exome sequencing: an example from hereditary deafness. *PLoS One*. 2012;7:e32000.
- Chong JX, Buckingham KJ, Jhangiani SN, Boehm C, Sobreira N, Smith JD, et al. The genetic basis of Mendelian phenotypes: discoveries, challenges, and opportunities. *Am J Hum Genet*. 2015;97:199–215.
- Ramzan M, Duman D, Hendricks LCP, Guo S, Mutlu A, Kalcioğlu MT, et al. Genome sequencing identifies coding and non-coding variants for non-syndromic hearing loss. *J. Hum. Genet*. 2023;68:1–13.

- Rehman AU, Santos-Cortez RLP, Drummond MC, Shahzad M, Lee K, Morell RJ, et al. Challenges and solutions for gene identification in the presence of familial locus heterogeneity. *Eur J Hum Genet* 2015;23:1207–15.
- Naz S, Imtiaz A, Mujtaba G, Maqsood A, Bashir R, Bukhari I, et al. Genetic causes of moderate to severe hearing loss point to modifiers. *Clin Genet* 2017;91:589–98.
- Richard EM, Santos-Cortez RLP, Faridi R, Rehman AU, Lee K, Shahzad M, et al. Global genetic insight contributed by consanguineous Pakistani families segregating hearing loss. *Hum Mutat* 2019;40:53–72.
- Lu Y, Zhou X, Jin Z, Cheng J, Shen W, Ji F, et al. Resolving the genetic heterogeneity of prelingual hearing loss within one family: Performance comparison and application of two targeted next-generation sequencing approaches. *J Hum Genet*. 2014;59:599–607.
- Das A, Dickinson DJ, Wood CC, Goldstein B, Slep KC. Crescerin uses a TOG domain array to regulate microtubules in the primary cilium. *Mol Biol Cell* 2015;26:4248–64.
- Perlaza K, Mirvis M, Ishikawa H, Marshall W. The short flagella 1 (SHF1) gene in *Chlamydomonas* encodes a Crescerin TOG-domain protein required for late stages of flagellar growth. *Mol Bio Cell* 2022;33:ar12.
- Belyantseva IA, Labay V, Boger ET, Griffith AJ, Friedman TB. Stereocilia: the long and the short of it. *Trends Mol Med* 2003;9:458–61.
- Miyoshi T, Belyantseva IA, Kitajiri S-I, Miyajima H, Nishio S-Y, Usami S-I, et al. Human deafness-associated variants alter the dynamics of key molecules in hair cell stereocilia F-actin cores. *Hum. Genet*. 2021;141:1–20.
- Riazuddin S, Ahmed ZM, Fanning AS, Lagziel A, Kitajiri S, Ramzan K, et al. Tricellulin is a tight-junction protein necessary for hearing. *Am. J. Hum. Genet*. 2006;79:1040–51.
- Van Hauwe P, Everett LA, Coucke P, Scott DA, Kraft ML, Ris-Stalpers C, et al. Two frequent missense mutations in Pendred syndrome. *Hum. Mol. Genet*. 1998;7:1099–104.
- Cassatella D, Howard SR, Acierno JS, Xu C, Papadakis GE, Santoni FA, et al. Congenital hypogonadotropic hypogonadism and constitutional delay of growth and puberty have distinct genetic architectures. *Eur. J. Endocrinol*. 2018;178:377–88.
- Vona B, Maroofian R, Mendiratta G, Croken M, Peng S, Ye X, et al. Dual Diagnosis of Ellis-van Creveld Syndrome and Hearing Loss in a Consanguineous Family. *Mol. Syndromol*. 2017;9:5–14.
- Yoshimura H, Miyagawa M, Kumakawa K, Nishio SY, Usami S. Frequency of Usher syndrome type 1 in deaf children by massively parallel DNA sequencing. *J. Hum. Genet*. 2016;61:419–22.
- Cengiz FB, Duman D, Sirmaci A, Tokgöz-Yılmaz S, Erbek S, Öztürkmen-Akay H, et al. Recurrent and private MYO15A mutations are associated with deafness in the Turkish population. *Genet. Test. Mol. Biomarkers*. 2010;14:543–50.

ACKNOWLEDGEMENTS

The authors thank all the members of hearing loss families for their participation and cooperation in the study.

AUTHOR CONTRIBUTIONS

Conceptualization: MR and MT, Data collection: MR, OA, AM, MFZ, CA, MT, Formal analysis: MR, GB, DD, Funding acquisition: MT, BV, KW, Writing original draft: MR and MT, Writing-review and editing: MR, OA, AM, MFZ, CA, GB, DD, TA, TK, KW, BV, DO, MT.

FUNDING

This work was supported by NIH R01DC009645 and R01DC012836 to MT and the German Research Foundation DFG VO 2138/7-1 grant 469177153 to BV and ANPCyT Argentina PICT-2021 GRF-TI-00422 to KW.

COMPETING INTERESTS

The authors declare no competing interests.

ETHICS DECLARATION

The study was approved by the Institutional Review Board at the University of Miami, USA, Ankara University Medical School Ethics Committee, Türkiye, Local Ethics Committee of Istanbul Medeniyet University, and Goztepe Training and Research Hospital Istanbul, Türkiye.

ADDITIONAL INFORMATION

Supplementary information The online version contains supplementary material available at <https://doi.org/10.1038/s41431-024-01562-6>.

Correspondence and requests for materials should be addressed to Mustafa Tekin.

Reprints and permission information is available at <http://www.nature.com/reprints>

Publisher's note Springer Nature remains neutral with regard to jurisdictional claims in published maps and institutional affiliations.

Springer Nature or its licensor (e.g. a society or other partner) holds exclusive rights to this article under a publishing agreement with the author(s) or other rightsholder(s); author self-archiving of the accepted manuscript version of this article is solely governed by the terms of such publishing agreement and applicable law.